Arxiv: 2407.14793

EPOCHS I. The Discovery and Star Forming Properties of Galaxies in the Epoch of Reionization at $6.5 < z < 18$ with PEARLS and Public JWST data

Christopher J. Conselice,[1] Nathan Adams,[1] Thomas Harvey,[1] Duncan Austin,[1] Leonardo Ferreira,[2] Katherine Ormerod,[1,3] Qiao Duan,[1] James Trussler,[1] Qiong Li,[1] Ignas Juodžbalis,[1,4,5] Lewi Westcott,[1] Honor Harris,[1] Louise T. C. Seeyave,[6] Asa F. L. Bluck,[7] Rogier A. Windhorst,[8] Rachana Bhatawdekar,[9] Dan Coe,[10] Seth H. Cohen,[8] Cheng Cheng,[11,12] Simon P. Driver,[13] Brenda Frye,[14] Lukas J. Furtak,[15] Norman A. Grogin,[16] Nimish P. Hathi,[16] Benne W. Holwerda,[17] Rolf A. Jansen,[8] Anton M. Koekemoer,[16] Madeline A. Marshall,[18] Mario Nonino,[19] Aaron Robotham,[13] Jake Summers,[8] Stephen M. Wilkins,[20] Christopher N. A. Willmer,[21] Haojing Yan,[22] and Adi Zitrin[15]

ABSTRACT

We present in this paper the discovery, properties, and a catalog of 1165 high redshift $6.5 < z < 18$ galaxies found in deep JWST NIRCam imaging from the GTO PEARLS survey combined with data from JWST public fields. We describe our bespoke, homogeneous reduction process and our analysis of these areas including the NEP, CEERS, GLASS, NGDEEP, JADES, and ERO SMACS-0723 fields covering a total of over 214 arcmin^2 imaged down to depths of ~ 30 mag. We give a description of our rigorous methods for identifying these galaxies, which involve the use of Lyman-break strength, detection significance criteria, visual inspection, and photometric redshifts probability distributions predominately at high redshift. Our sample is a robust and highly pure collection of distant galaxies from which we also remove brown dwarf stars, and calculate completeness and contamination from simulations. We include a summary of the basic properties of these $z > 6.5$ galaxies, including their redshift distributions, UV absolute magnitudes, standard stellar masses, and star formation rates. Our study of these young galaxies reveals a wide range of stellar population properties as seen in their observed and rest-frame colors which we compare to stellar population models. This mix of systems indicate a range of star formation histories, dust content, AGN and/or nebular emission. We find that a strong trend exists between stellar mass and $(U - V)$ color, as well as the existence of the 'main-sequence' of star formation for galaxies as early as $z \sim 12$. This indicates that despite the complexities of galaxy formation, stellar mass, or an underlying variable correlating with stellar mass, is driving galaxy formation, in agreement with simulation predictions. We also discuss unusual and very high redshift candidates at $z > 12$ in our sample. Finally, we compare our galaxy counts in redshift to models of galaxy formation, finding a significant observed excess of galaxies at the highest redshifts compared to models at $z > 12$, revealing a tension between predictions and our observations.

Introduction:

The earliest galaxies represent the building blocks of the universe as they are the seeds of the structures we observe today.
Pre-JWST: HST Y-band (F105W); z < 8.5 Lyman break galaxies (LBGs)
Early JWST data: candidate LBGs at z > 12
JADES-GS-z13-0 (Curtis-Lake+22); JADES-GS-z14-0,1 (Carniani+24)

EPOCHS sample: A large area (avoiding cosmic variance) analysis with the **same reductions**, galaxy detection, and analysis processes. → **1165 galaxies at z > 6.5**
The EPOCHS series papers (II-IV): the role of galaxies in the early Universe; how reionization occurred and when and how the first galaxies assembled.

Data reduction and products:

11 of the deepest JWST fields in PEARLS, GLASS, NGDEEP, JADES, CEERS, SMACS-0723 data

PEARLS

Field	Area (arcmin^2)	HST/ACS_WFC F606W	F814W	JWST/NIRCam F090W	F115W	F150W	F200W	F277W	F335M	F356W	F410M	F444W
NEP	57.32	28.74	-	28.50	28.50	28.50	28.65	29.15	-	29.30	28.55	28.95
El Gordo*	3.90	-	-	28.23	28.25	28.18	28.43	28.96	-	29.02	28.45	28.83
MACS-0416*	12.3	-	-	28.67	28.62	28.49	28.64	29.16	-	29.33	28.74	29.07
Clio*	4.00	-	-	28.12	-	28.07	28.21	28.675	-	28.91	-	28.71
CEERS	66.40	28.6	28.30	-	28.70	28.60	28.89	29.20	-	29.30	28.50	28.85
CEERSP9	6.08	28.31	28.32	-	29.02	28.55	28.78	29.20	-	29.22	28.50	29.12
SMACS-0723*	4.31	-	-	28.75	-	28.81	28.95	29.45	-	29.55	-	29.28
GLASS	9.76	-	-	29.14	29.11	28.86	29.03	29.55	-	29.61	-	29.84
NGDEEP HST-S	1.28	29.20	28.80	-	29.78	29.52	29.48	30.28	-	30.22	-	30.22
NGDEEP HST-D	4.03	30.30	30.95	-	29.78	29.52	29.48	30.28	-	30.22	-	30.22
JADES Deep GS	22.98	29.07	-	29.58	29.78	29.68	29.72	30.21	29.58	30.17	29.64	29.99

30.07 in JADES paper (0.15")

SExtractor makes image masks, then put 200 apertures to calculate NMAD and derive depth
The depths listed are at 5σ in AB magnitudes, measured in 0.16" radius apertures
'Stage 1': Reprocessing all of the NIRCam imaging from their lowest-level, raw form obtained from the MAST database with the up-to-date NIRCam pipeline & calibrations. Subtract templates of 'wisps' (large scale artefacts in the imaging caused by rogue light).
'Stage 2': 1/f noise correction (appears as stripes in JWST data; https://jwst-docs.stsci.edu/known-issues-with-jwst-data/nircam-known-issues/nircam-1-f-noise-removal-methods#gsc.tab=0); Background subtraction utilizing 'photutils'
'Stage 3': A final mosaic is produced and align the WCS of GAIA DR3. Then, aligning them to the F444W image. Finally, pixel-match the images to the F444W image with the final scale of 0.03 arcseconds/pixel.
A systematic way across all fields, to avoid inhomogenous data quality, methodology, and systematics to directly compare data in different fields.

Construct catalogs of objects by **SExtractor** in **dual-image mode**, using an inverse variance weighted stack of the F277W, F356W and F444W bands.

Column Name	Unit	Description
IDs, Positions, Fluxes and local depths		
ID		Unique catalogue ID, consisting of number and fieldname
ALPHA_J2000	degree	Right ascension
DELTA_J2000	degree	Declination
FIELDNAME		Field/pointing the galaxy is in
FLUX_APER_**BAND**	nJy	Aperture corrected flux in 0.16 arcsec radius apertures
FLUXERR_APER_**BAND**	nJy	Local-depth derived flux error from NMAD of 200 nearby empty apertures
sigma_**BAND**		SNR of detection in 0.16 arcsec aperture
local_depth_**BAND**	AB Mag	5σ local depth from NMAD of flux in 200 nearby empty apertures
unmasked_**BAND**	Boolean	Whether galaxy is masked in **BAND**
auto_corr_factor_**BAND**		Correction factor in **BAND** for flux outside 0.16 arcsec aperture
Photometric Redshifts and Selection		
zbest		Photometric redshift using EAZY
zbest_l1		-1σ photometric redshift uncertainty using EAZY
zbest_u1		$+1\sigma$ photometric redshift uncertainty using EAZY
chi2_best		χ^2 of EAZY fit
PDF_integral_eazy		$\int_{0.94\times \mathrm{zbest}}^{1.06\times \mathrm{zbest}} \mathrm{PDF}(z)dz$ - Integral of EAZY posterior redshift PDF
zbest_lowz		Photometric redshift using EAZY, with $z_{\max} = 6$
chi2_best_lowz		χ^2 of EAZY fit, with $z_{\max} = 6$
UV Properties		
M_UV*	AB Mag	Absolute UV mag in 100Å tophat at 1500Å rest-frame flux at redshift zbest
M_UV_u1	AB Mag	
M_UV_l1	AB Mag	
BETA_UV		UV slope $f \propto \lambda^{\beta}$ (see Austin et al. (2024)).
BETA_UV_l1		
BETA_UV_u1		
SFR_UV*	$M_\odot\ yr^{-1}$	
SFR_UV_l1	$M_\odot\ yr^{-1}$	
SFR_UV_u1	$M_\odot\ yr^{-1}$	
Sample identifiers		
certain_by_eye	Boolean	Visual inspection of cutout and SED boolean
EPOCHS_II	Boolean	Used in EPOCHS II (UV LF)
EPOCHS_III	Boolean	Used in EPOCHS III (UV β and dust)
EPOCHS_IV	Boolean	Used in EPOCHS IV (SMF)

χ^2<3: "robust"; χ^2<6: "good"

Photometry-based: direct and not based on the SED fits

Circular apertures flux of 0.32" diameter, balance the use of high-signal pixels when computing fluxes and avoid dependence on a PSF model correction.

Photometric Redshifts: "tweak fsps qsf v12 v3" templates + Set 1 and Set 4 of the templates in Larson et al. (2022), which provides bluer-rest frame colors and high equivalent width emission lines (young ages).

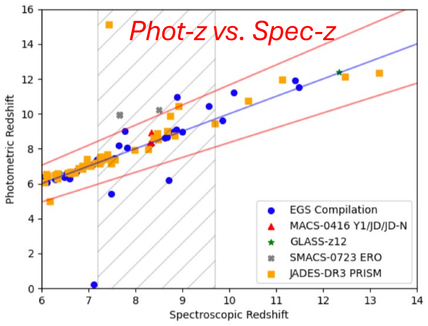

Sample selection criertia:

1. > 5σ significance in the two bands redward of the estimated Lyman break and with non-detections, or less than 3σ detections, in all bands (minimum of a single band) bluewards.
2. The integration of the PDF within the range of 10% of the peak photometric redshift PDF value must include at least 60% of the total PDF integral. (X: bimodal solutions)
3. An additional fit with EAZY with a maximum redshift z = 6 allowed in the fits. χ^2 between the high−z and low−z solutions be ≤ −4.
4. Objects with sizes significantly smaller than a PSF (half light radius < 1.5 pix) are removed.
5. All objects are subjected to visual inspection by multiple authors to identify and remove any artifacts or contaminated sources

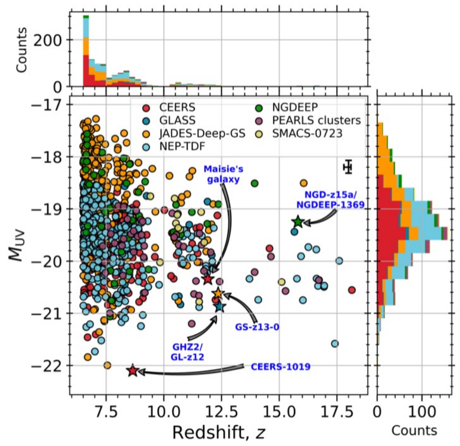

Results:

1. A large diversity of galaxy UV brightness consistent with the LF through the first 500 Myr.
Very luminous galaxies up to z ~ 18 → No obvious evolution in the upper limit of UV brightness.

2. A general trend of downsizing, such that the most massive galaxies at 8.5 < z < 10.5 have the lowest specific star formation rates, the oldest ages, and the highest masses.

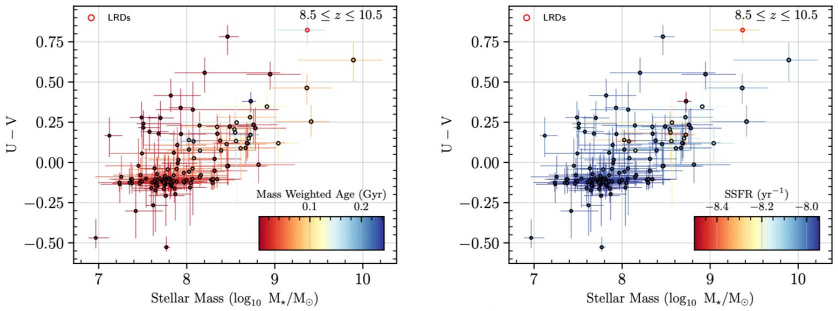

3. SFMS at z > 6.5
The scatter in the shorter time-scale (10 Myr) can range over a factor of ~ 30, whilst for the longer time-scale (100 Myr) the range is over a factor of ~ 5.
SFRs are higher compared to most studies, a factor of ~ 5 higher than the z = 9 SFMS from HST.

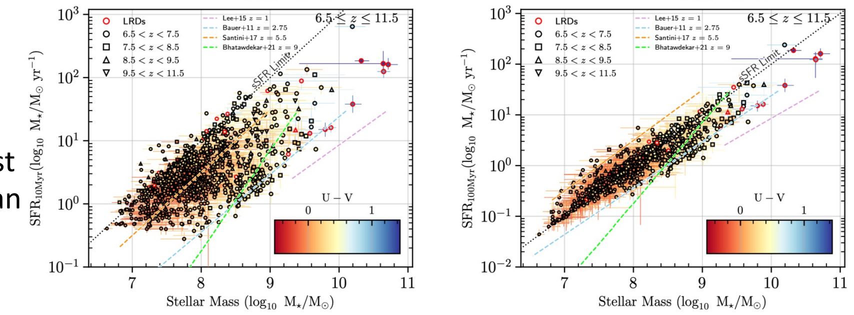

4. A generally good agreement between some galaxy properties, compared with simulations, including those from FLARES
5. Selection bias not only from cosmic variance, but also from redshift/magnitude, depending on the depth and filter.
No bias in the colors of galaxies in different fields, that overall, each field is finding similar galaxies

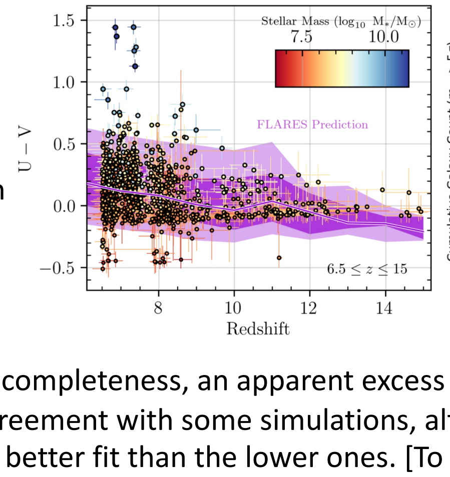

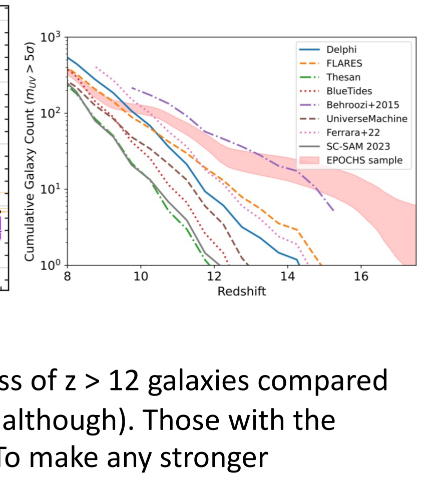

6. Even without a correction for incompleteness, an apparent excess of z > 12 galaxies compared with models. (At z < 10, a good agreement with some simulations, although). Those with the highest predicted abundances are better fit than the lower ones. [To make any stronger statements will require future JWST spectroscopy]